Thermochimica Acta, 144 (1989) 123–139
Elsevier Science Publishers B.V., Amsterdam – Printed in The Netherlands

KINETIC STUDY OF ISOTHERMAL AND CONTINUOUS HEATING CRYSTALLIZATION IN $Se_{100-x}Bi_x$ ($x \leqslant 8$) GLASSES

A. MUÑOZ and F.L. CUMBRERA

Departamento de Física de la Materia Condensada, Facultad de Física, Ap° 1065, Sevilla (Spain)

(Received 3 August 1988)

ABSTRACT

Calorimetric studies of chalcogenide glasses $Se_{100-x}Bi_x$ obtained by vacuum co-evaporation have been performed by isothermal and continuous heating experiments in a Perkin Elmer DSC-2C calorimeter. The Se–Bi system displays stable immiscibility and this could be an explanation for the small number of papers in the literature. Results obtained in both isothermal and non-isothermal experiments are interpreted with the same set of kinetic parameters. Our data are in agreement with the kinetic Johnson–Mehl–Avrami–Erofe'ev equation. The interpretation of the Se–Bi crystallization can best be understood by reference to phase separation phenomena.

1. INTRODUCTION

It is well recognized that non-crystalline materials show reduced thermal stability. These materials generally share a number of interesting properties related to the absence of long-range order which are lost when they evolve toward crystalline phases, i.e. when temperature is raised. Therefore, a comprehensive study of the crystallization mechanisms and the kinetics of the transformation would be very useful in establishing the applicability range of these materials.

Bi-doped amorphous chalcogenides and, particularly, the $Se_{100-x}Bi_x$ system have been obscured for a long time in spite of their striking electrical properties [1–3]. In fact, the $Se_{100-x}Bi_x$ system is presented [4] as an example of stable liquid immiscibility. Furthermore, in the phase diagram in Fig. 1 we can see a monotectic region around the most relevant zone: the Se rich region. Such difficulties can justify the small number of papers dealing with the non-crystalline $Se_{100-x}Bi_x$ system. In order to achieve homogeneity in the zone of x between 2 and 27 we need to bypass the immiscibility gap by means of condensation from the vapour phase. According to Fleury et al. [5], above 3 at.% Bi the $Se_{100-x}Bi_x$ samples were no longer amorphous. The introduction of a third element, such as I [6] or Ge [7] is a method of

0040-6031/89/$03.50

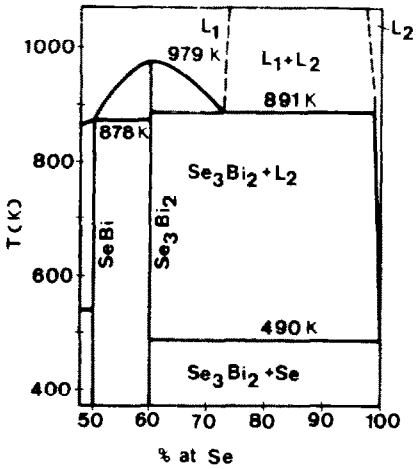

Fig. 1. Phase diagram of the Se–Bi system.

avoiding the phase separation problem. Recently, the possibility was suggested [8] of extending the region in which the system behaves as a homogeneous amorphous solution by suitable control of the preparative conditions. In previous work [9] we have succeeded in preparing amorphous and homogeneous thin films of the $Se_{100-x}Bi_x$ system for $x < 5$, and have investigated the features of its structural short-range order by means of electron diffraction experiments. In this paper we report on a differential scanning calorimetric (DSC) study of the crystallization kinetics of this system for $x \leqslant 8$. The crystallization experiments were performed by both isothermal and continuous heating measurements of the transformation rate.

2. EVALUATION OF KINETIC PARAMETERS AND MODEL RELATIONS

Information concerning the kinetics of the crystallization of amorphous materials can be inferred from very different experimental techniques. The direct methods, such as transmission electron microscopy (TEM) are advantageous in that they are a straightforward way of obtaining the kinetic parameters. However, they suffer from severe limitations: (i) They are normally concerned with very thin films where the proximity between free surfaces can give rise to biasing of the crystallization mechanism; for example, surface-induced crystallization processes (SIC) are able to mask the bulk-induced crystallization (BIC). (ii) The smallness of the analyzed area may be not representative of the whole of the material. Therefore, indirect methods such as thermoanalytical ones are widely used to characterize the amorphous–crystal transition.

The interpretation of DSC experiments has been controversial for several reasons. On the one hand, kinetic equations for the transformation rate,

which have been derived for isothermal conditions, have been carelessly handled for non-isothermal experiments [10–12]. On the other hand, if the principle of separation of variables is assumed for the rate of the process in non-isothermal conditions

$$d\alpha/dt = K(T)f(\alpha) \tag{1}$$

α being the transformed fraction, different choices hold for the T or α-dependent parts. It is almost always the case that $K(T)$ is represented by an Arrhenius law

$$K(T) = K_0 \exp\left(-\frac{E}{K_b T}\right) \tag{2}$$

where K_0 is the preexponential factor and E the effective activation energy.

However, Barandiaran et al. [13] have shown that for many polymeric and metallic glasses the Vogel–Fulcher expression

$$K(T) = K_{ov} \exp\left(\frac{1}{\alpha_f (T - T_0)}\right) \tag{3}$$

α_f being the free volume expansion coefficient and T_0 the ideal liquid-glass temperature, gives a more adequate description of the crystallization of these glasses. Particularly, the unrealistically high values for K_0 often obtained are avoided. With regard to the α-dependent part, different forms for the $f(\alpha)$ function which fulfill the mathematical requirements of eqn. (1) are possible. However, the most customary model relation for solid-state reactions is

$$f(\alpha) = n(1-\alpha)[-\ln(1-\alpha)]^{(n-1)/n} \tag{4}$$

which corresponds to the Johnson–Mehl–Avrami–Erofe'ev (JMAE) equation, where n is the kinetic exponent. Ingenious methods have been proposed to investigate the most suitable analytical model for $f(\alpha)$ or to fit the n exponent if the JMAE equation is accepted. The starting point is generally eqn. (1) or its integral form. In that respect, Tang [14] has noted the difficulty of reliably determining $f(\alpha)$ even from low-scatter non-isothermal data when the effect of this function is masked by the T-dependence. Thus at least two experiments are required to study the kinetics of a transformation: an isothermal experiment to identify the model relation $f(\alpha)$, and a dynamic experiment to obtain K_0 and E. More recently, baró and co-workers [15,16] have successfully obtained the kinetic parameters of the crystallization of some chalcogenide and metallic glasses by the choice of an adequate "master representation" which is highly discriminative with regard to the shape of $f(\alpha)$, namely $\ln f(\alpha) : -\ln(1-\alpha)$. Two assumptions are implicit in their work: crystallization is thermally activated following Arrhenius behaviour and the same set of kinetic parameters fit both isothermal and non-isothermal experiments.

A paper of MacCallum and Tanner [17] was the beginning of a rather extensive discussion about understanding the dependence of α upon time and temperature. These authors have suggested the following expression for the transformation rate under non-isothermal conditions

$$\frac{d\alpha}{dt} = \left(\frac{\partial \alpha}{\partial t}\right)_T + \left(\frac{\partial \alpha}{\partial T}\right)_t \frac{dT}{dt} \tag{5}$$

which indicates that $\alpha(t, T)$ is a true constitutive equation and α is independent of the T–t path. The application of eqn. (5) along the JMAE expression yields

$$\frac{d\alpha}{dt} = K(T)n(1-\alpha)[-\ln(1-\alpha)]^{(n-1)/n}\left[1 + \frac{E}{K_b}\frac{T-T_0}{T^2}\right] \tag{6}$$

when $T = T_0 + \dot{T}t$, and which includes in the last bracket a general correction term to the transformation rate equation [18]. Kemény and Granasy [19,20] and other authors have shown that there is no reason for this correction term, provided that the transformed fraction is not a state function of t and T, as it is also dependent on the T–t path.

The most commonly used methods to obtain the activation energy E are based upon the measurements of the peak temperatures T_p under different heating rates $q = \dot{T}$. Kissinger [21], starting from the empirical model relation $f(\alpha) = (1-\alpha)^n$ showed that a plot of $\ln[q/T_p^2]$ versus $1/T_p$ should yield a straight line from whose slope E is calculated. Other authors [22,23] have found justification for the Kissinger formula, even starting from the JMAE model relation. A different approach was tried by Marseglia and Davis [24] who, considering $\alpha(t, T)$ as a state function and also the peak condition $d^2\alpha/d^2t = 0$, deduced that a linear dependence holds between $\ln[q/T_p]$ and $1/T_p$, so allowing the determination of E.

In light of the above considerations we have outlined the following strategy for a quantitative analysis of the kinetic parameters in the crystallization of the $Se_{100-x}Bi_x$ system.

(i) From isothermal experiments we obtain the kinetic exponent n which accounts for the crystallization mechanism. Since the JMAE equation can be expressed as

$$\alpha = 1 - \exp[-(Kt)^n] \tag{7}$$

a plot of $\log[-\ln(1-\alpha)]$ versus $\log t$ provides the n exponent.

(ii) Continuous heating experiments are analyzed on the basis of the Kissinger relation

$$\ln\left(q/T_p^2\right) = \ln(K_0 K_b/E) - (E/K_b T_p) \tag{8}$$

In this way we derive the E and K_0 kinetic parameters, which are compared to those obtained by means of the Marseglia expression.

(iii) On the assumption of eqn. (1) and the Arrhenius behaviour of $K(T)$ we can derive the activation energy by means of a plot of $\ln(d\alpha/dt)$ versus $1/T$, for constant α. The agreement between isothermal and continuous heating regimes allow us to use the method proposed in refs. 15 and 16. Therefore we find confirmation 'a posteriori' of the JMAE and Arrhenius behaviour for $f(\alpha)$ and $K(T)$.

3. EXPERIMENTAL

Thin films of the $Se_{100-x}Bi_x$ system with $x \leqslant 8$ and about 1.5 μm thick were prepared by vacuum co-evaporation of the components from two separate allumina crucibles. The elements were of 5N purity (Johnson-Matthey) and the residual pressure was 2×10^{-4} Pa. Glass substrates were used and kept at room temperature during deposition. The control of the thickness and the composition was carried out during the deposition by means of a quartz microbalance and the final composition was determined by the electron microprobe method. More details of the experimental arrangement have been described elsewhere [9].

Electron diffraction experiments guarantee the non-crystalline character of the samples. The crystallization kinetics have been studied by means of thermoanalytical methods. Differential scanning calorimetry experiments were performed in a Perkin Elmer DSC-2C with an intracooler device under pure argon atmosphere. The samples were stripped from their substrates and placed in aluminium sample holders for calorimetric experiments. Calibrations of temperature and areas were carried out by measuring the transformation curve of melting of pure In and Pb and the areas subtended under the peaks were measured with a semiautomatic image analyzer Kontron MOP-30.

4. RESULTS AND DISCUSSION

The results for pure Se have been reported in a previous paper [25]. In the present work we consider the $Se_{100-x}Bi_x$ system for $x \leqslant 8$ although the Se data are useful as reference.

4.1. Isothermal experiments

Figure 2 shows the isothermal thermograms corresponding to $T = 365$ K and the different compositions studied. Figure 3 shows the variation of $\log[-\ln(1-\alpha)]$ with $\log t$ for different values of x and for the selected annealing temperatures. The values obtained for n are represented in Table 1. A correct interpretation of these kinetic exponents is strongly connected

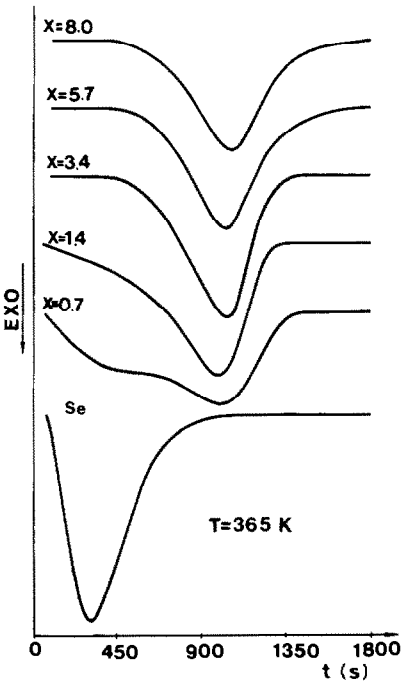

Fig. 2. DSC traces obtained in isothermal mode at 365 K for different values of x in the $Se_{100-x}Bi_x$ system.

to the phase separation phenomena. In this manner, it is meaningful to refer to Fig. 4 which shows the evolution with x of a dynamic DSC experiment with a constant heating rate of 20 K min^{-1} for samples of the same mass. We can appreciate the glass transition, the crystallization and, on a different scale, the melting. These thermograms reveal a single glass transition whose temperature, T_g, rises with the Bi content; this increase indicates that the system at room temperature behaves as a solid solution and is not multiphase. The endotherms are due to room ambient relaxation effects on T_g. However, for the compositions in the region of the immiscibility gap a drop is observed just above T_g. This exothermic effect corresponds, according to Myers and Berkes [4], to an irreversible structural separation in the metastable liquid above T_g. An easy experiment can bring light to elucidate this behaviour: the samples heated through T_g are cooled back into the glass regime and then reheated through T_g. This subsequent heating reveals (Fig. 5) a significant decrease into T_g and the loss of the exothermal drop, indicating a glass containing less Bi. Furthermore, this remnant glassy phase holds a fixed Bi content and its subsequent crystallization gives rise to a very similar crystallization peak, irrespective of x inside the immiscibility gap. This phase separation above T_g has been observed [26] by means of transmission electron microscopy (TEM) experiments: from the initial homogeneous solid solution a decomposition process takes place giving rise to

two phases whose compositions correspond to the limits of the immiscibility gap. Afterwards, the Bi-rich phase undergoes a monotectoid reaction giving rise to the precipitation of crystalline Se_3Bi_2 and Se, whereas the Bi-poor phase ($\simeq$ 2 at.%) remains amorphous.

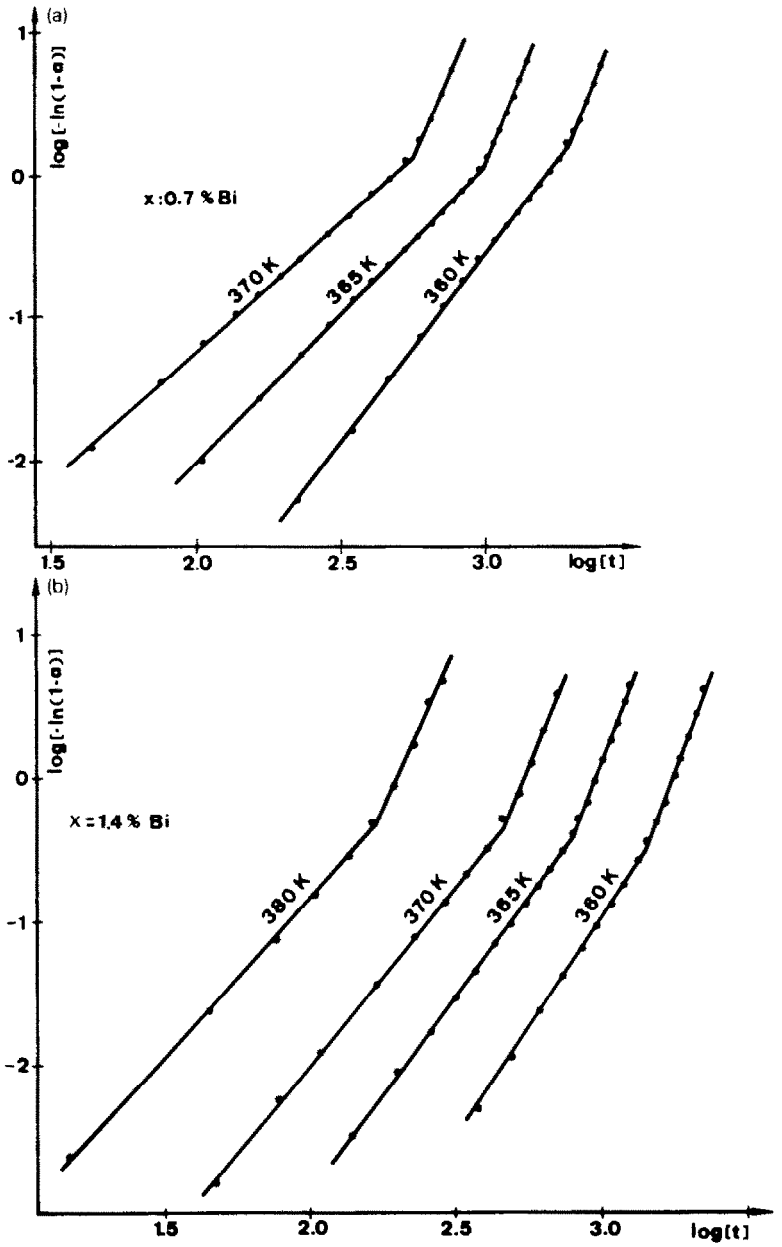

Fig. 3. Avrami plots at various annealing temperatures: (a) $x = 0.7$, (b) $x = 1.4$, (c) $x = 3.4$, (d) $x = 5.7$, (e) $x = 8.0$.

In the light of these results the following explanation is concluded for the kinetic exponents of Table 1. Two cases may be distinguished.

(i) For x below the immicibility gap we observe a first stage very similar to the crystallization of pure Se (it is interesting to see the anomalous

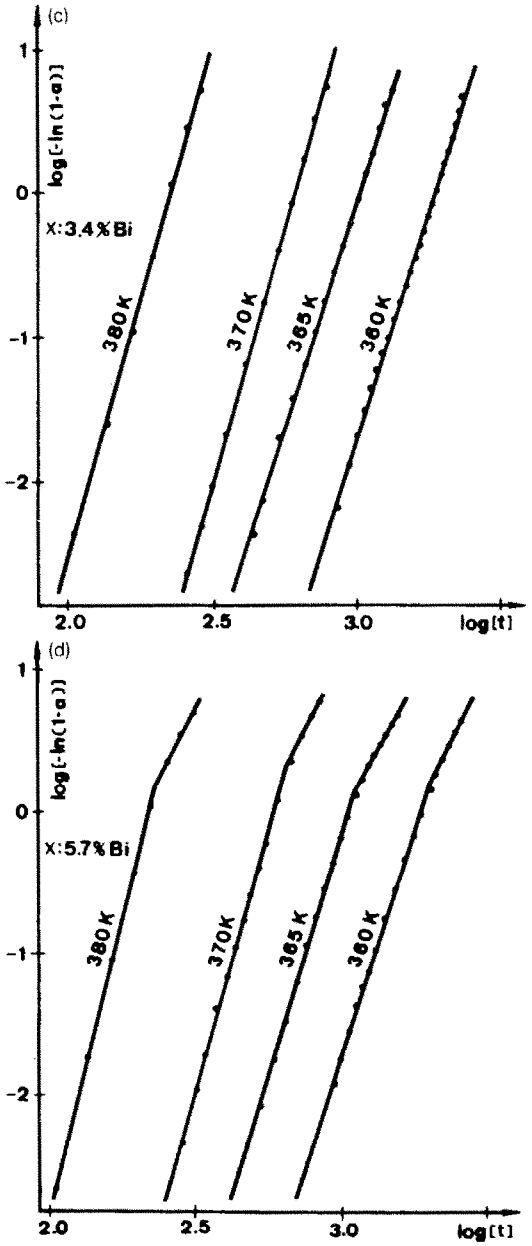

Fig. 3 (continued).

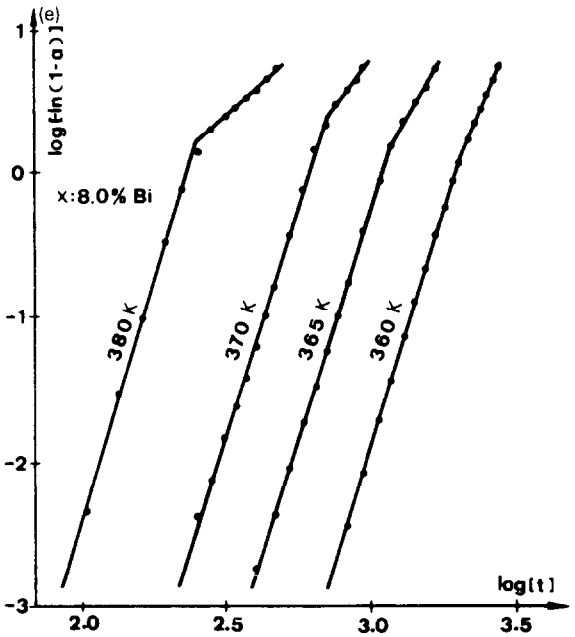

Fig. 3 (continued).

behaviour of the crystallization peak for $x = 0.7$ and 1.4 in Figs. 2 and 4). The value $n \simeq 3$ observed for the lower annealing temperatures is consistent with a three-dimensional growth of heterogeneous crystallites either pre-existent in the amorphous phase or more probably arising from the formation of seed crystals above the glass transition temperature. The drop down to $n \simeq 2$ for higher temperatures probably indicates an increase of the initial size of the heterogeneous nuclei, a_0, so that $a_0 \simeq e$ (e being the thickness of the sample), inducing to a two-dimensional growth. With regard to the second stage of the crystallization, the higher values found for n (between 4.5 and 5.4) may be explained assuming that the precipitation of crystalline Se yields to a progressive rise of the Bi content in the remaining glassy

TABLE 1

Values obtained for the kinetic exponent of the JMAE equation for various annealing temperatures, T, and different compositions in the $Se_{100-x}Bi_x$ system

T (K)	(at.% Bi)				
	0.7	1.4	3.4	5.7	8.0
360	2.8 → 5.1	3.1 → 5.4	6.3	6.3 → 4.1	6.5 → 4.9
365	2.3 → 5.2	2.7 → 5.4	6.2	6.7 → 3.8	6.4 → 3.6
370	2.0 → 4.6	2.5 → 5.0	7.2	7.3 → 4.1	6.4 → 2.7
380		2.2 → 4.5	7.3	8.2 → 4.0	6.7 → 1.8

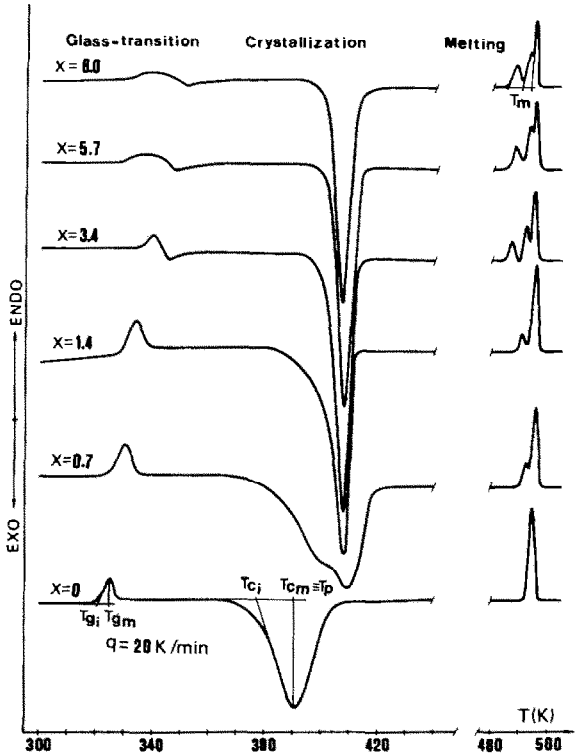

Fig. 4. The effect of x in the $Se_{100-x}Bi_x$ system on a continuous heating experiment performed at $q = 20$ K min^{-1}.

phase. When the boundary of the immiscibility gap is attained the phase separation phenomena take place giving rise to a strong dependence upon time of the nucleation rate. According to Christian [10], $n > 4$ values are expected in this case.

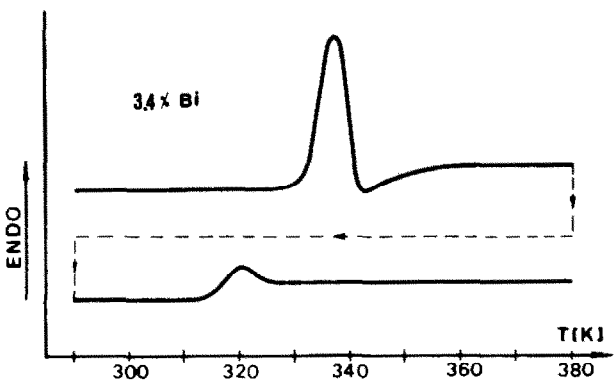

Fig. 5. Consecutive thermal analysis around the glass transition region for $x = 3.4$.

(ii) For x inside the immiscibility gap phase separation in the isothermal experiments takes place immediately from the beginning. In this way, the high values of n are measured even for short times. For $x > 3.4$, once the phase separation is concluded a final stage is observed with $n \simeq 4$, corresponding to a homogeneous nucleation process with the nucleation rate slightly dependent upon time. Indeed, once the heterogeneous processes are exhausted, homogeneous ones becomes predominant.

4.2. Continuous heating experiments

The activation energies of the crystallization processes were determined by Kissinger's peak shift method. Figure 6 shows the Kissinger plot for the different compositions studied and Table 2 summarizes the results obtained for E and K_0 besides other data measured from the thermograms. No significant differences in the values of E and K_0 were observed for the different compositions except for a slight rise with x which is within the calculated error interval.

The key to interpreting the kinetic results in the $Se_{100-x}Bi_x$ system appears to lie in the phase separation phenomena. As mentioned in Section 4.1, the glassy phase which remains after the decomposition process and whose composition corresponds to the limit of the immiscibility gap explains the constancy of E and K_0 with x.

Otherwise, Kissinger plots obtained after several ageing times do not reveal significant changes in E and K_0, unlike the behaviour observed for

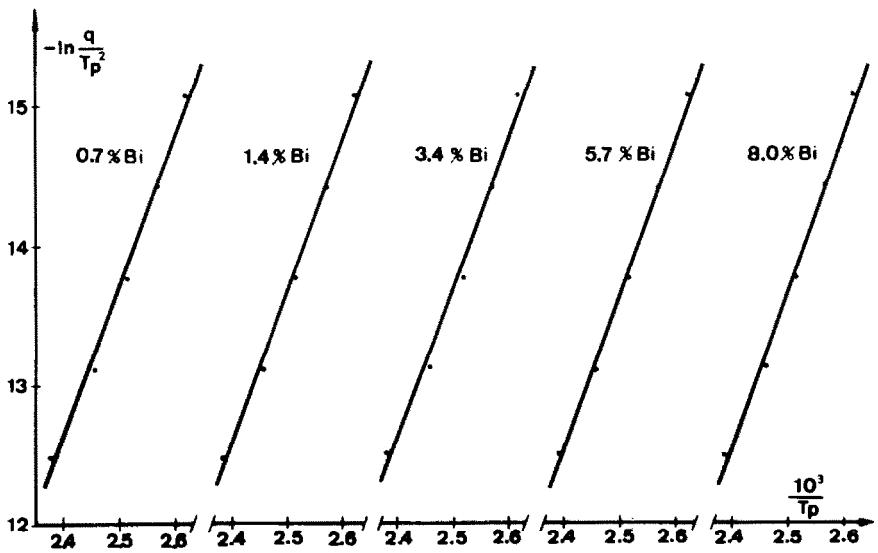

Fig. 6. Kissinger's plots for different compositions in the $Se_{100-x}Bi_x$ system.

TABLE 2

Values of E and K_0 for the $Se_{100-x}Bi_x$ system with other data of interest

x (at.% Bi)		0.7	1.4	3.4	5.7	8.0
E (eV at.$^{-1}$)		0.93	0.93	0.93	0.96	0.97
K_0 (s^{-1})		6.6×10^9	7.4×10^9	6.7×10^9	1.6×10^{10}	1.9×10^{10}
$q=10$ K min^{-1}	Tg_i(K)	322.1	327.5	331.5	328.3	332.2
	Tg_m(K)	324.8	330.7	335.9	333.9	336.8
	Tc_i(K)	378.8	378.5	392.6	392.3	392.9
	Tc_m(K)	397.8	397.0	397.0	396.7	397.3
	T_m(K)	488.7	488.7	484.1	484.1	484.1
		492.4	492.4	488.7	488.7	488.7
				492.4	492.4	492.4
ΔH_c (kJ mol^{-1})		3.9 ± 0.4	3.8 ± 0.4	3.5 ± 0.3	3.5 ± 0.3	3.3 ± 0.3

pure Se [26]. This result indicates that the possible role of Bi as branching additive imposes supplementary constraints for the relaxation of Se chains.

Besides Kissinger's method we have tried the previously mentioned method of Marseglia in order to obtain the basic kinetic parameters. The results of both approaches are very similar except for a slight increase in the E value (about 5%) and a decrease in ln K_0 (about 10%).

On the other hand, the region around 490 K in Fig. 4 shows several endothermic peaks corresponding to the melting. The presence of even three melting peaks for $x > 2$ make manifest the existence of crystalline selenium in different compositional environments.

4.3. Kinetic analysis from master curves

It is well known that $f(\alpha)$ is the function which reflects the mechanisms of crystallization. In fact, the analysis of $f(\alpha)$ is useful if we want to distinguish which one of the several kinetic models can describe the crystallization process. Several classical kinetic equations are presented in Table 3. Some equations, labelled R, correspond to a reaction process controlled by diffusion across the interface. Others, labelled D, correspond to reactions controlled by diffusion through the sample. The consideration of a nucleation process prior to crystal growth is taken into account in the previously mentioned JMAE kinetic model of order n, Fn. The aforementioned models are presented in Fig. 7.

In our analysis we use the method of Baró and co-workers [15,16] which has been outlined in Section 2. We have used the whole sequence of values of α in the range 0.05–0.95 and analyzed eqn. (1) for each scanning rate in non-isothermal experiments, and for each temperature in isothermal experiments. By combining eqns. (1) and (2) we obtain the expression

$$\ln[K_0 f(\alpha)] = \ln\frac{d\alpha}{dt} + \frac{E}{K_b T} \tag{9}$$

TABLE 3

Theoretical kinetic model equations considered

Kinetic model	$f(\alpha)$
R1 Polanyi–Wigner	α^0
R2 Shrinking cylinder	$2(1-\alpha)^{1/2}$
R3 Shrinking sphere	$3(1-\alpha)^{2/3}$
D1 Tamman	$1/2\ \alpha^{-1}$
D2 Valensi	$[-\ln(1-\alpha)]^{-1}$
D3 Ginstling–Brounstein	$3/2[(1-\alpha)^{-1/3}-1]^{-1}$
F*n* Avrami–Erofeev	$n(1-\alpha)[-\ln(1-\alpha)]^{(n-1)/n}$

where K_0 is only a shift factor in the representation of Fig. 7. The validity of the above equation is established by the linear behaviour of the plot of $\ln \mathrm{d}\alpha/\mathrm{d}t$ versus $1/T$ for fixed values of α (Fig. 8) irrespective of the isothermal or continuous heating regime. The slopes of these straight lines allow us to obtain the activation energy E (Table 4). Using E and $\mathrm{d}\alpha/\mathrm{d}t$, obtained from our experimental data, we obtain from eqn. (9) the pairs of values for $\ln[K_0 f(\alpha)]$ and $\ln(1-\alpha)$ which we present in Fig. 9. In spite of some scatter of the points the overall pattern is sufficiently good to justify the assumption that the crystallization process is independent of heating

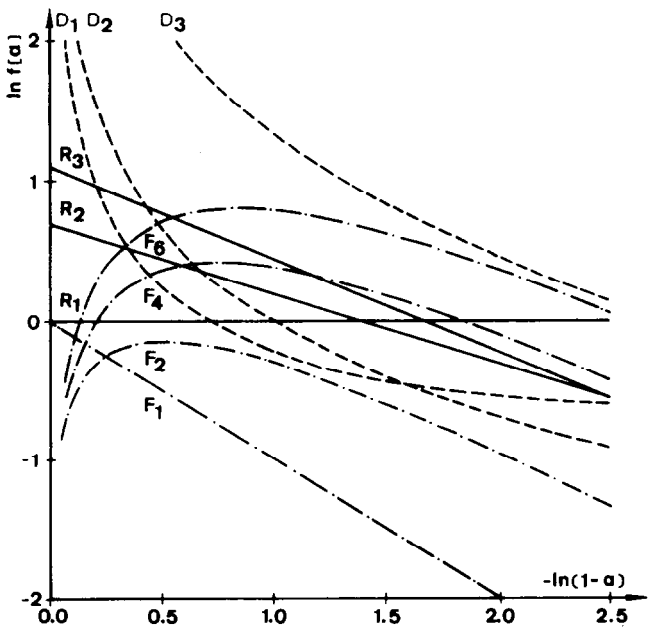

Fig. 7. Master curves $\ln f(\alpha)$ vs. $\ln(1-\alpha)$ for the different kinetic equations summarized in Table 3.

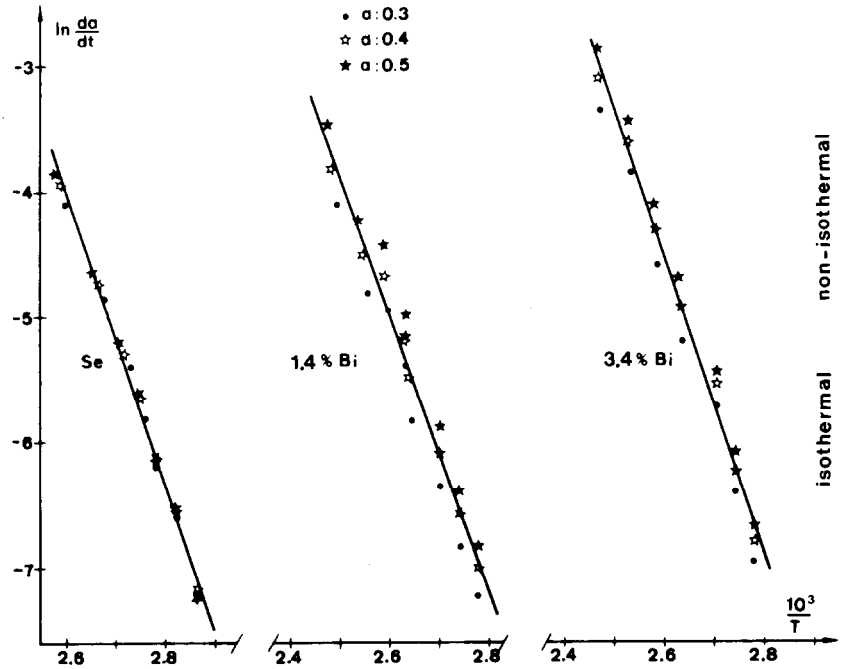

Fig. 8. Plots of $d\alpha/dt$, in logarithmic form, versus $1/T$ for fixed transformed fractions and isothermal and continuous heating data.

rate, at least in the range $0 \leqslant q \leqslant 20$ K min^{-1}. This independence of the thermal history can justify the similarity between the E values obtained by the Kissinger or the Marseglia method. As expected, the kinetic equation that gives the best fit is the JMAE one. By means of a least-squares fit we have determined the values of n and K_0 for the compositions studied ($x = 0$, 1.4, 3.4). As we can deduce from the results, shown in Table 4, the n values obtained by this procedure come to be an averaged kinetic exponent over the different ageing temperatures and over the different stages of crystallization. However, for those samples with $x = 1.4$ it was not possible to find a single fit to the data: this fact makes it evident that the crystallization is dominated by at least two independent processes with very unequal n exponents. On this basis we have carried out a fit corresponding to both

TABLE 4

Least-squares calculated values of n, K_0 and E for some compositions in the $Se_{100-x}Bi_x$ system

x (at.% Bi)	0	1.4	3.4
E (eV at.$^{-1}$)	1.00	0.95	1.02
n	2.0	2.7–5.4	6.8
K_0 (s^{-1})	2.5×10^{11}	1.5×10^{10}	1.1×10^{11}

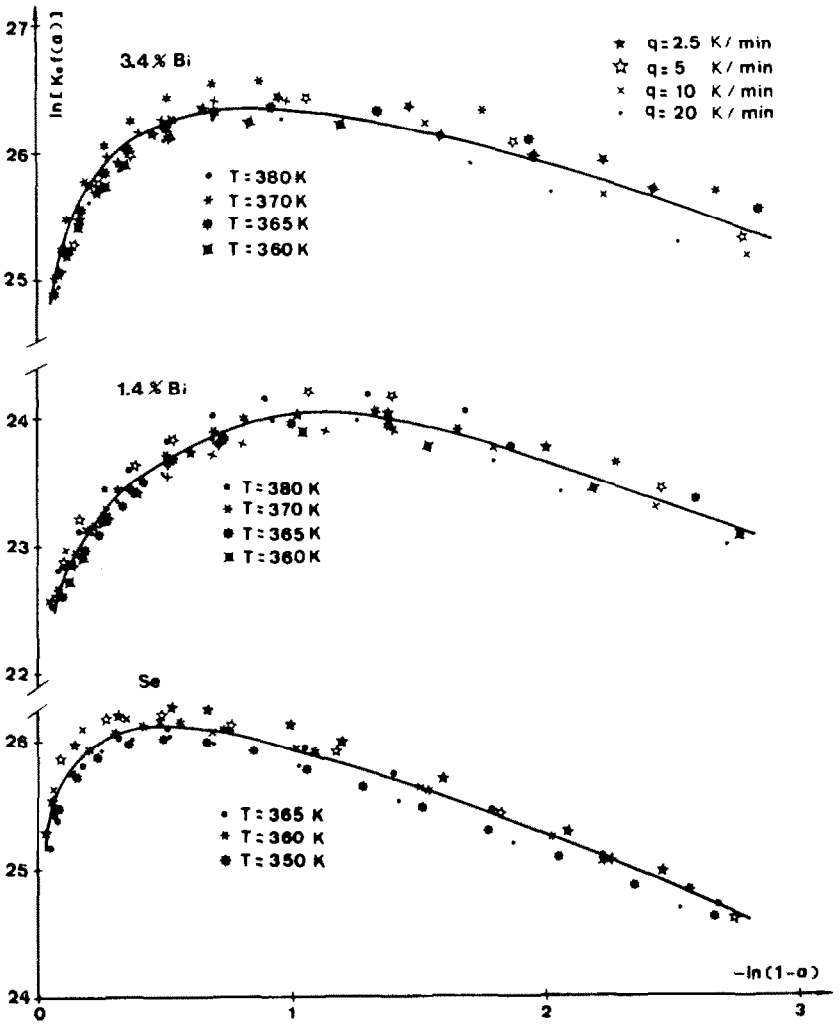

Fig. 9. Plots of $\ln[K_0 f(\alpha)]$ vs. $\ln(1-\alpha)$ for samples with different compositions. Points correspond to experimental data in isothermal and non-isothermal experiments whereas the continuous lines are the best theoretical fit to the JMAE equation.

lower α values ($\alpha < 0.3$) which yields $n = 2.7$ and higher α values ($\alpha > 0.6$) yielding $n = 5.4$. It is remarkable to observe that both values fall within the interval previously obtained from isothermal experiments for the two stages found for crystallization (initial segregation of crystalline Se and phase separation).

4.4. Crystallization enthalpy

Besides the kinetic parameters reported above, we have evaluated the enthalpy change, ΔH_c, related to the crystallization process. The results

obtained, shown in Table 2, do not depend significantly on the isothermal or non-isothermal character of the experiment.

An observed trend is the slight decrease in ΔH_c as the Bi content increases. This decrease is more important for compositions inside the immiscibility gap, possibly because a small part of the material crystallized at the end of the glass transition as a consequence of phase separation.

5. SUMMARY

We have studied the crystallization process of the non-crystalline system $Se_{100-x}Bi_x$ for $x \leqslant 8$ by means of isothermal and continuous heating experiments. The results obtained reveal that crystallization is mainly controlled by the phase separation phenomena.

We have verified the validity of eqns. (1) and (2) and the form of JMAE for the model relation $f(\alpha)$. The values of the main kinetic parameters such as n, E and K_0, were obtained. The values of n are interpreted and discussed for the compositions studied and compared with the results of TEM observations.

The kinetic parameters are shown to be independent of both temperature and thermal sample history, at least for the temperature interval analyzed. This fact explains why non-isothermal experiments provide complete information on the crystallization process.

REFERENCES

1 J.C. Schottmiller, D.L. Bowman and C. Wood, J. Appl. Phys., 39 (1968) 1666.
2 N. Tohge, T. Minami and M. Tanaka, J. Non-Cryst. Solids, 37 (1980) 23.
3 T. Takahashi, J. Non-Cryst. Solids, 44 (1981) 239.
4 M.B. Myers and J.S. Berkes, J. Non-Cryst. Solids, 8–10 (1972) 804.
5 G. Fleury, A. Hamou, C. Lhermite and C. Viger, Phys. Status Solidi A, 83 (1984) K103.
6 W.J. Hillegas and J.M. Neyhart, J. Non-Cryst. Solids, 27 (1978) 347.
7 K.L. Bathia, J. Non-Cryst. Solids, 54 (1983) 173.
8 J.M. Saiter, Doctoral Thesis, Rouen, 1986.
9 A. Muñoz, F.L. Cumbrera and R. Márquez, Mater. Lett., 7 (1988) 138.
10 J.W. Christian, Theory of Transformations in Metals and Alloys, 2nd edn., Pergamon Press, Oxford, 1975.
11 D.W. Henderson, J. Non-Cryst. Solids, 30 (1979) 301.
12 D.W. Henderson, J. Therm. Anal., 15 (1979) 325.
13 J.M. Barandiaran, I. Telleria, A. Rivacoba and J. Colmenero, Thermochim. Acta, 63 (1983) 225.
14 T.B. Tang, Thermochim. Acta, 58 (1982) 373.
15 S. Suriñach, M.D. Baró, M.T. Clavaguera-Mora and N. Clavaguera, J. Non-Cryst. Solids, 58 (1983) 209.
16 M.D. Baró, S. Suriñach, M.T. Clavaguera-Mora and N. Clavaguera, J Non-Cryst. Solids, 69 (1984) 105.

17 J.R. MacCallum and J. Tanner, Nature (London), 225 (1970) 1127.
18 J. Norwisz, Thermochim. Acta, 25 (1978) 123.
19 T. Kemény and L. Gránásy, J. Non-Cryst. Solids, 68 (1984) 193.
20 L. Gránásy and T. Kemény, Thermochim. Acta, 42 (1980) 289.
21 H.E. Kissinger, Anal. Chem., 29 (1959) 1702.
22 T. Ozawa, Bull. Chem. Soc. Jpn., 38 (1965) 1881.
23 H.S. Chen, J. Non-Cryst. Solids, 27 (1978) 257.
24 E.A. Marseglia and E.A. Davis, J. Non-Cryst. Solids, 50 (1982) 13.
25 A. Muñoz, F.L. Cumbrera, A. Conde and R. Márquez, Thin Solid Films, 149 (1987) L73.
26 A. Muñoz, Doctoral Thesis, Sevilla, 1988.